EXTENDED THOMAS–FERMI CALCULATIONS FOR HOT NUCLEAR SYSTEMS

Matthias BRACK
Institut für Theor. Physik, Universität Regensburg
Universitätsstraße 31, D-8400 Regensburg, FRG

ABSTRACT

We review the extended Thomas-Fermi theory for systems at finite temperature and present numerical results of applications to semi-infinite nuclear matter and to hot finite nuclei.

1. INTRODUCTION

The semiclassical density variational method using the extended Thomas-Fermi (ETF) density functionals and Skyrme-type effective nuclear interactions has become a competitive economical tool for calculating average nuclear ground-state properties and deformation energies. (See ref.[1)] for a recent review.) Quantitative agreement with the averaged results of - much more time consuming - Hartree-Fock (HF) calculations is reached. Hereby the inclusion of the second- and fourth-order gradient corrections to the ETF kinetic energy functional with their correct coefficients and the corresponding contributions from variable effective nucleon masses and spin-orbit potentials have been shown to be crucial, in particular when calculating fission barriers.[1,2)]

The growing interest in the properties of hot nuclear systems, stimulated by recent progress both in astrophysics and heavy ion reactions, have necessitated the generalization of the ETF theory to finite temperatures, i.e. in particular the determination of the temperature-dependent gradient corrections to the functionals of the free (kinetic)

energy $F[\rho]$ and of the entropy $S[\rho]$. This has recently been achieved[3,4]. The new functionals have been shown to become quantum-mechanically exact at nuclear temperatures $T \geq 3$ MeV where the shell effects are washed out.[4] (At lower temperatures they do not describe correctly the shell fluctuations.) Therefore, at the corresponding excitation energies, which nowadays can easily be reached in heavy ion reactions, the density variational method using these functionals becomes completely equivalent to the microscopical HF method, however at appreciably lower computational costs.

In the present paper we shall briefly review the finite-temperature ETF theory in section 2. In sect. 3 we apply the density variational method to semi-infinite nuclear matter in which case the fourth-order, nonlinear Euler differential equation has been solved numerically.[4] Two situations are discussed:

a) the case of phase equilibrium between the gas and the condensed (liquid) phase at finite pressure, such as it might be encountered in a collapsing star and thus is of interest in the astrophysical context;
b) the case of zero pressure in the region of the condensed phase, such as will be the situation of an isolated, hot compound nucleus, formed in a heavy ion collision, which is metastable (similarly to a superheated liquid drop).

The latter situation is studied in sect. 4 in variational calculations for finite hot nuclei, and the question of a limiting temperature at which the nucleus ceases to be bound, is discussed. We finally also summarize some recent calculations for sum rules for nuclear monopole and dipole giant resonances using the variational finite-temperature ETF densities.

Much of the material presented here is the result of various collaborations which will be referred to at the appropriate places. I take the occasion here to thank J. Bartel, C. Guet, J. Meyer, P. Quentin and E. Strumberger for their important contributions.

2. THE FINITE-TEMPERATURE ETF THEORY

We shall only quote here the key results; for derivations and more detailed expressions we refer to refs.[1,4] All quantities given in this section hold for one kind of nucleons.

2.1 The ETF Density Functionals

The local density functionals-including gradient corrections - for the kinetic energy $K[\rho]$, the entropy $S[\rho]$ and the free energy $F[\rho]$

$$F[\rho] = K[\rho] + \int V(\vec{r})\rho(\vec{r})\,d^3r - T\,S[\rho] \tag{1}$$

of a system of Fermions moving in a local potential $V(\vec{r})$ at temperature T (measured in energy units with $k \equiv 1$) with density $\rho(\vec{r})$, are most conveniently derived with the help of a semiclassical $\hbar$-expansion of the density matrix $\rho(\vec{r},\vec{r}')$ originally due to Wigner and Kirkwood.[5] (For alternative derivations of the same $\hbar$-expansion, see refs.[6,7]) At finite temperature, the Wigner transform of $\rho(\vec{r},\vec{r}')$, i.e. the Wigner function, becomes[4]

$$f_{ETF}(\vec{p},\vec{q}) = n_T(\lambda - H_{CL}) - \frac{\hbar^2}{8m}\Delta V(\vec{q})\, n_T''(\lambda - H_{CL}) + \\ + \frac{\hbar^2}{24m}\left\{[\vec{\nabla}V(\vec{q})]^2 + \frac{1}{m}(\vec{p}\cdot\vec{\nabla}_q)^2 V(\vec{q})\right\} n_T'''(\lambda - H_{CL}) + O(\hbar^4), \tag{2}$$

where $n_T(E)$ is the Fermi function

$$n_T(E) = [1 + \exp(-E/T)]^{-1} \tag{3}$$

and $n_T''(E)$, $n_T'''(E)$, etc. are its derivatives, and H_{CL} is the classical Hamilton function

$$H_{CL}(\vec{p},\vec{q}) = \frac{p^2}{2m} + V(\vec{q}). \tag{4}$$

From $f_{ETF}(\vec{p},\vec{q})$ eq. (2), all local densities of interest (density ρ, kinetic energy density τ, entropy density σ, etc.) can be derived easily. Eliminating the Fermi energy λ, the potential V and its

derivatives, one obtains after some tedious algebra[3,4] the ETF functional for the free energy

$$F_{ETF}[\rho] = \int d^3r \left\{ V(\vec{r})\rho(\vec{r}) + \mathcal{F}_{TF}[\rho] + \mathcal{F}_2[\rho] + \mathcal{F}_4[\rho] + \ldots \right\}, \quad (5)$$

where

$$\mathcal{F}_{TF}[\rho] = T\eta\rho - \frac{1}{3\pi^2}\left(\frac{2m}{\hbar^2}\right)^{3/2} T^{5/2} J_{3/2}(\eta), \quad (6)$$

$$\mathcal{F}_2[\rho] = \frac{\hbar^2}{2m}\zeta(\eta)\frac{(\vec{\nabla}\rho)^2}{\rho}, \quad (7)$$

$$\mathcal{F}_4[\rho] = \left(\frac{\hbar^2}{2m}\right)^2 \frac{1}{T}\left[\vartheta_1(\eta)\frac{(\Delta\rho)^2}{\rho} + \vartheta_2(\eta)\frac{\Delta\rho(\vec{\nabla}\rho)^2}{\rho^2} + \vartheta_3(\eta)\frac{(\vec{\nabla}\rho)^4}{\rho^3}\right]. \quad (8)$$

Hereby the parameter η is a function of ρ and T: $\eta = \eta(\rho,T)$, defined by the (unique) solution of the equation

$$\rho = \rho(\vec{r}) = \frac{1}{2\pi^2}\left(\frac{2m}{\hbar^2}\right)^{3/2} T^{3/2} J_{1/2}(\eta). \quad (9)$$

The so-called Fermi integrals $J_\mu(\eta)$ in eqs. (6) and (9) are defined by

$$J_\mu(\eta) = \int_0^\infty \frac{x^\mu}{1 + e^{x-\eta}}\, dx. \quad (10)$$

The coefficients $\zeta(\eta)$ and $\vartheta_i(\eta)$ in eqs. (7,8) are universal, analytical functions of η defined in terms of $J_{1/2}(\eta)$ and its derivatives; they can be computed once for all and are given in ref.[4] Since all local densities (ρ,τ,σ etc.) are analytical functions at $T > 0$ (as long as $V(\vec{r})$ is analytical), one has no turning point problem as it arises[1] at $T = 0$, so that the functional $F_{ETF}[\rho]$ is strictly valid also in the classically forbidden regions.

The functional $S_{ETF}[\rho]$ for the entropy is obtained from $F_{ETF}[\rho]$ eq. (5) simply by the canonical thermodynamical relation

$$S[\rho] = -\left.\frac{\partial F[\rho]}{\partial T}\right|_{\rho=\text{const.}} \tag{11}$$

Once $F_{ETF}[\rho]$ and $S_{ETF}[\rho]$ are known, the kinetic energy functional $K_{ETF}[\rho]$ is trivially found from eq. (1).

In refs.[1,4] it was shown that in the limit $T \to 0$, $S_{ETF}[\rho]$ goes to zero like T and $K_{ETF}[\rho]$ goes over into the old kinetic energy functional known at $T = 0$[1,6,7]

$$K_{ETF}[\rho] \xrightarrow[T\to 0]{} \frac{\hbar^2}{2m}\int d^3r \left\{ \varkappa \rho^{5/3} + \frac{1}{36}\frac{(\vec{\nabla}\rho)^2}{\rho} + \tau_4[\rho] + \ldots \right\} \tag{12}$$

with $\varkappa = 3/5(3\pi^2)^{2/3}$ and the form of $\tau_4[\rho]$ given first by Hodges.[8] Since the limit $T \to 0$ can be taken locally at any point in space where $\rho(\vec{r}) > 0$, this constitutes the first rigorous proof that the old ETF functional for $\tau[\rho]$ at T=0 is valid also beyond the classically allowed region.

According to the theorem by Hohenberg and Kohn[9] and its generalization to $T > 0$ by Mermin[10], the functionals $K[\rho]$ and $S[\rho]$ are universal and independent of the local potential $V(\vec{r})$. Due to the semiclassical nature of the ETF model and its underlying $\hbar$-expansion, the ETF functionals cannot reproduce correctly the fluctuating shell effects in the total energies or entropies; they apply, however, to the shell-averaged quantities. This has been demonstrated numerically in refs.[11, 12] with the help of microscopically Strutinsky-averaged densities at T=0. (See ref.[13] for a model case where average and shell fluctuating parts are separated analytically.)

A well-known result of the smearing of the Fermi level at finite temperatures is the disappearence of the shell effects. In HF calculations for finite nuclei at $T > 0$ it was shown [14,15] that independently of the nucleon numbers, the shell effects disappear at about $T \simeq 2.5$ to 3 MeV. At and beyond these temperatures, the energy and all other expectation values are smooth functions of deformation and nucleon numbers,and one should expect the semiclassical functionals to

become appropriate. Indeed, it was shown in ref.[4] in model calculations for a deformed harmonic oscillator potential that for $T \gtrsim 3$ MeV, the above ETF functionals yield the exact quantum-mechanical free energy or entropy within less than 0.1 % in terms of the exact density $\rho(\vec{r})$. (The convergence of the series in eq. (5) is so fast that the sum of sixth and higher order terms can be expected to contribute less than 0.1 %.) Thus, for all practical purposes, the ETF functionals up to fourth order become quantum-mechanically exact at temperatures where the shell effects vanish.

The $\hbar$-expansion and the ETF functionals can, with some algebraic effort, be extended to velocity-dependent one-body potentials, such as they occur in HF calculations with SKyrme-type effective nuclear forces[16]

$$\hat{H} = -\vec{\nabla} \cdot \frac{\hbar^2}{2m^*(\vec{r})} \vec{\nabla} + V(\vec{r}) - i \vec{W}(\vec{r}) \cdot (\vec{\nabla} \times \vec{\sigma}) \qquad (13)$$

with a variable effective mass and a spin-orbit potential. For the corresponding contributions to the second-order gradient corrections at $T \geq 0$, see refs.[1,4] and to the fourth-order corrections at T=0, see ref.[7].

2.2 Density Variation And The Euler Equation

Using the above semiclassical functionals, the total HF energy of a nucleus can be expressed as a local functional of the proton and neutron densities alone, if a Skyrme-type force is used. For a finite-range force, density matrix expansion (DME) techniques[17] can be used to arrive at similar local functionals. For the following discussion, we neglect for simplicity the difference between protons and neutrons and omit the Coulomb interaction. The total free energy is then

$$F_{HF} = \int d^3r \, \mathcal{F}[\rho(\vec{r})], \qquad (14)$$

where the free energy density functional $\mathcal{F}[\rho]$ contains the sum of all

integrands in eq. (5) after, however, replacing $V(\vec{r})\rho(\vec{r})$ by the HF potential energy density. Including gradient corrections to the ETF functionals up to fourth order in $\hbar$, we can write $\mathcal{F}[\rho]$ in the following form:

$$\mathcal{F}[\rho] = \mathcal{F}_\infty(\rho) + s(\rho)(\vec{\nabla}\rho)^2 + g(\rho)(\vec{\nabla}\rho)^4 + h(\rho)(\Delta\rho)^2 + \ell(\rho)\Delta\rho(\vec{\nabla}\rho)^2. \qquad (15)$$

Hereby $\mathcal{F}_\infty(\rho)$ is the free energy density for infinite nuclear matter as a function of the density ρ; s,g,h and ℓ are functions of ρ containing the T-dependent coefficients in eqs. (7,8) and those parameters of the force which describe its nonlocal or finite-range components.

A nucleus at a finite temperature is not stable unless it is in thermodynamical equilibrium with a surrounding nucleon gas. The quantity to be minimized is therefore the Gibbs free energy, which leads to the variational equation

$$\frac{\delta}{\delta\rho(\vec{r})}\int d^3r\left\{\mathcal{F}[\rho] - \lambda\rho + P_0\right\} = 0. \qquad (16)$$

Hereby the chemical potential λ is the Lagrange multiplier which keeps the particle number constant, and P_0 is the finite external pressure necessary to maintain the phase equilibrium. Doing the variation in eq. (16) leads to the Euler differential equation

$$\frac{d\mathcal{F}_\infty(\rho)}{d\rho} - 2s(\rho)\Delta\rho - \frac{ds(\rho)}{d\rho}(\vec{\nabla}\rho)^2 + \frac{\delta\mathcal{F}_4[\rho]}{\delta\rho} = \lambda; \qquad (17)$$

the last term on the ℓ.h. side is the variational derivative of the fourth-order gradient term eq. (8) - i.e. the sum of the last three terms in eq. (15) - which contains up to fourth derivatives of $\rho(\vec{r})$. Eq. (17) is thus a highly nonlinear fourth-order differential equation which in general is very difficult to solve. The boundary condition is such that far outside the nucleus, where the gas has a constant

density ρ_g , the integrand in eq. (16) must vanish, so that

$$P_o = \lambda \rho_g - \mathcal{F}_\infty(\rho_g) . \tag{18}$$

This means just that P_o is the pressure of an infinitely extended gas with constant density ρ_g. This is the situation which may approximately be reached locally in a collapsing massive star, where condensed nuclei exist in phase equilibrium with a surrounding gas of nucleons (and leptons).

The situation is different for an isolated, hot nucleus such as it may be formed in a heavy ion collision. Since there is no external pressure, the nucleus will evaporate nucleons and thus be metastable, similar to a superheated liquid drop (see, e.g. ref.[18]). The variation in eq. (16) must therefore be done at $P_o = 0$. This leads to the same Euler equation as eq. (17) above, however with different boundary conditions. Before we discuss these and some corresponding numerical equations in sect. 4, we shall in the following section turn to the semi-infinite case which corresponds to the limit of a very large nucleus where curvature effects can be neglected.

3. SEMI-INFINITE NUCLEAR MATTER

We discuss here an infinite two-phase system in which condensed (liquid) nuclear matter is separated from a nucleon gas by the z-plane. We only consider the symmetric (isoscalar) case with $\rho_n = \rho_p = \frac{1}{2}\rho$. The interface is described by a one-dimensional density profile $\rho(z)$ with the limiting values

$$\rho(-\infty) = \rho_o , \quad \rho(+\infty) = \rho_g . \tag{19}$$

The finite quantity which is made stationary in this case is the (Gibbs) free interface energy per unit area (see also ref.[19]) which we call here simply the surface tension σ as in the T = 0 case:

$$\sigma = \int_{-\infty}^{+\infty} \{ \mathcal{F}[\rho(z)] - \lambda \rho(z) + P_o \} \, dz . \tag{20}$$

Variation of σ with respect to $\rho(z)$ leads again to the same Euler equation (17), except that the gradients are replaced by d/dz (see ref.[4] for its full form). Since the z variable does not show up explicitely - in consistency with translational invariance - one can transform the equation with the substitution

$$p(\rho) = [\rho'(z)]^2 \tag{21}$$

into a differential equation for $p(\rho)$. It can be integrated once analytically to the second-order equation[4]

$$\mathcal{F}_\infty - \lambda\rho + P_0 = s p + (3g - \ell')p^2 + \\ + \tfrac{1}{4}\ell\,(p')^2 - p\,(\ell p')'; \tag{22}$$

the primes denote here derivatives with respect to ρ. Eq. (22) can be solved numerically with standard methods, using the appropriate boundary conditions (see below). In terms of the solution $p(\rho)$, the inverse surface profile $z(\rho)$ can then be determined through eq. (21) by a simple quadrature:

$$z(\rho) = -\int_{\rho_g}^{\rho} \frac{1}{+\sqrt{p(\rho')}}\, d\rho' + C; \tag{23}$$

the integration constant C is irrelevant. The surface tension σ (20) can be expressed directly in terms of $p(\rho)$ as[4]

$$\sigma = \int_{\rho_g}^{\rho_0} \frac{d\rho}{+\sqrt{p(\rho)}} \left\{ \tfrac{4}{3}\left[\mathcal{F}_\infty(\rho) - \lambda\rho + P_0\right] + \tfrac{2}{3} s(\rho) p(\rho) \right\}. \tag{24}$$

3.1 The Equilibrium Case

In the case of phase equilibrium, one has the equality of the chemical potential at the constant limiting densities eq. (19) on either side

$$\lambda = \mathcal{F}_\infty'(\rho_g) = \mathcal{F}_\infty'(\rho_0) \tag{25}$$

and pressure equilibrium

$$P_o = \lambda \rho_o - \mathcal{F}_\infty(\rho_o) = \lambda \rho_g - \mathcal{F}_\infty(\rho_g) . \qquad (26)$$

It is then easily seen from eqs. (17) and (22) that the boundary conditions for $p(\rho)$ are

$$p(\rho_o) = p(\rho_g) = p'(\rho_o) = p'(\rho_g) = 0. \qquad (27)$$

The four constants λ, P_o, ρ_o and ρ_g are at each temperature determined by eqs. (25) and (26) which lead to the well-known Maxwell construction. The solutions are illustrated in Figs. 1 and 2 for the Skyrme force SkM*.[1,20] Fig. 1 shows the pressure isotherms. At each temperature (except T = 5 MeV), the solutions for ρ_o and ρ_g are indicated by dots connected with a dashed horizontal line. The critical temperature is seen to be T_{crit} = 14.6 MeV. In Fig. 2 we show P_o, ρ_o

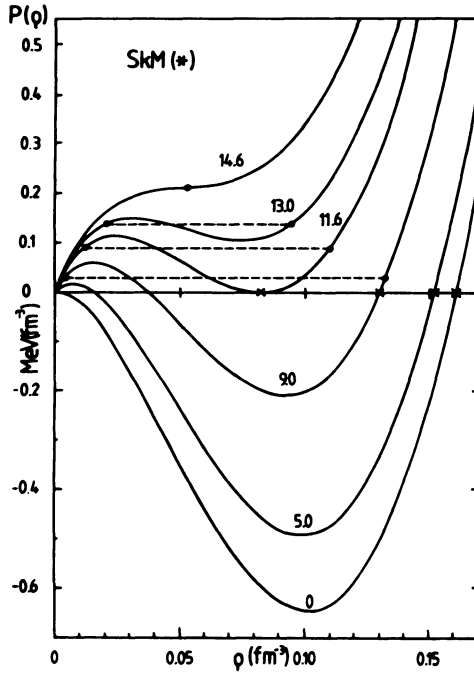

Figure 1:
Pressure isotherms for infinite nuclear matter obtained with the SkM* force. The temperature is given in MeV. From ref.[1)]

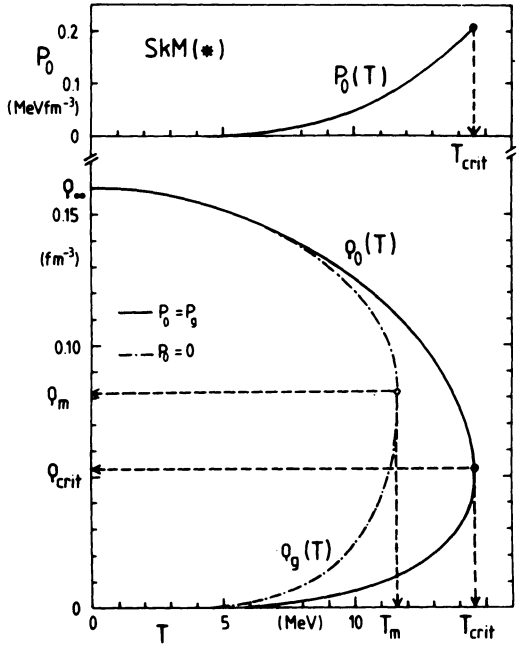

Figure 2:
Equilibrium pressure p_0, liquid density ρ_0 and gas density ρ_g from fig. 1 versus temperature T. Case of phase equilibrium (at p_0): solid lines. Metastable case (with pressure $p_0 = 0$ in liquid phase): dashed lines (see text in sect. 3.2 below). From ref.[1].

and ρ_g versus temperature T by the solid lines. The critical density ρ_{crit} is seen to be close to one-third of the saturation density ρ_∞ at T = 0.

Eqs. (22), (25)-(27) have been solved numerically in ref.[4]. The resulting profiles $\rho(z)$ are shown in Fig. 3 for the same SkM* force by the solid lines. The dashed lines are variational trial densities of the following form:

$$\rho(z) = \rho_g + \frac{\rho_0 - \rho_g}{(1 + e^{z/\alpha})^\gamma} \quad . \tag{28}$$

The parameters α and γ where hereby determined by minimizing σ eq. (20). The densities eq. (28) are seen to approximate the exact ones extremely well. The corresponding values of the surface tension σ agree within less than 1 % at low T and within less than 0.1 % at $T \gtrsim 5$ MeV. This gives a nice confirmation of earlier variational calculations for finite nuclei[1] using generalized Fermi functions of the form (28).

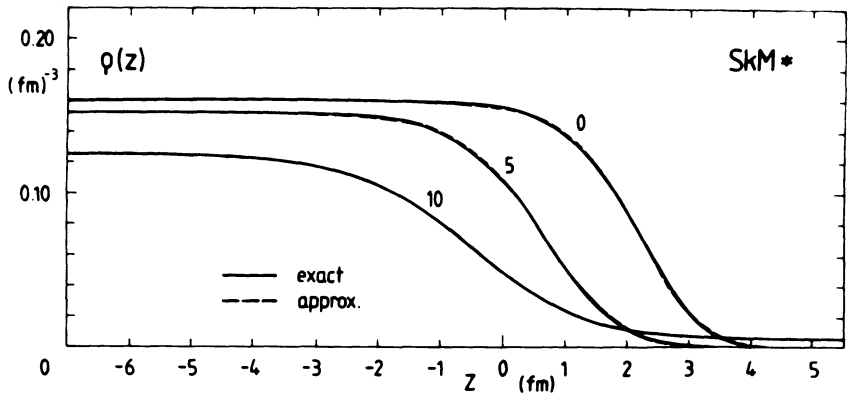

Figure 3:
Density profiles ρ(z) for infinite nuclear matter (SkM* force) at three temperatures (in MeV). Solid lines: exact numerical solution. Dashed lines: optimized trial densities eq. (28). From ref.[4].

From the numerical solutions, one can easily determine the symmetric liquid-drop parameters of the free energy of a nucleus in equilibrium with its surrounding gas

$$F = a_v A + a_s A^{2/3} + a_c A^{1/3} + \ldots$$
$$+ \text{asymmetry terms} + \text{Coulomb energy} . \qquad (29)$$

The surface energy coefficient is $a_s = 4\pi r_o^2 \sigma$ with $r_o = (4\pi\rho_o/3)^{-1/3}$; for the coefficient a_c see refs.[1,4]. In Fig. 4 we show the parameters a_s and a_c versus temperature by the solid lines. a_c contains also the so-called compression energy[1,21] (about - 2.8 MeV at T = 0). Both parameters go to zero at the critical temperature T_{crit} where they loose their meaning. The asymmetric (isovector) liquid-drop parameters can be obtained analogously by solving two coupled Euler equations for two densities $\rho_n(z)$ and $\rho_p(z)$. Their evaluation is the object of a forthcoming publication.[22]

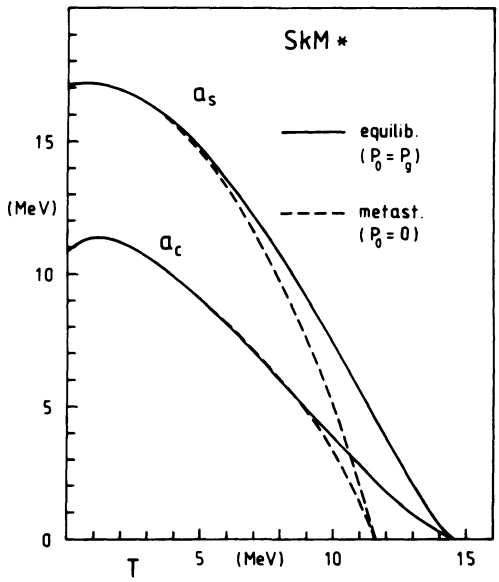

Figure 4:
Liquid drop parameters a_s (surface energy) and a_c curvature energy) versus temperature T (SkM* force). Solid lines: phase equilibrium. Dashed lines: metastable case (see sect. 3.2). From ref.[22].

3.2 The Metastable Case ($P_o = 0$)

If we want to simulate the situation of an isolated, metastable nucleus in the limit $A \to \infty$, we have to require $P_o = 0$ in the condensed phase i.e. at $z = -\infty$. The limiting density ρ_o is then just the saturation density found at each temperature from the equation

$$\mathcal{F}'_\infty(\rho_-) = \lambda = \frac{\mathcal{F}_\infty(\rho_-)}{\rho_-} \,. \tag{30}$$

However, as was pointed out already by Stocker and Burzlaff in TF calculations at $T > 0$[23], there is no other solution to the Euler equation (17) at $P_o = 0$ with a constant density (except the trivial case $\rho = 0$ at $T = 0$; for $T > 0$, $\mathcal{F}'_\infty(\rho)$ diverges logarithmically for $\rho \to 0$!). Instead, Stocker and Burzlaff found[23] that integrating outwards from the saturation density ρ_o, the solution $\rho(z)$ decreases until it reaches a minimum at a finite distance from the surface, say at z_o,

at which the density is nonzero:

$$\rho'(z_o) = 0, \tag{31}$$

$$\rho(z_o) = \rho_g > 0. \quad (T>0) \tag{32}$$

Beyond z_o, the profile $\rho(z)$ increases again, so that the solution must be cut at $z = z_o$. The density ρ_g at z_o is such that the integrand of eq. (20) (with $P_o = 0$) vanishes there:

$$\mathcal{F}_\infty(\rho_g) = \lambda \rho_g. \tag{33}$$

The same qualitative solutions are also found if the ETF gradient corrections are included in the Euler equation[1,24]: there exists a finite distance z_o at which eqs. (31) - (33) are fulfilled. The non-zero difference between $\mathcal{F}_\infty'(\rho_g)$ and λ in eq. (17) is made up by nonzero values of some of the higher derivatives of $\rho(z)$ at z_o. If only the second-order gradient corrections are taken into account (i.e. if $\mathcal{F}_4[\rho]$ is neglected), one finds $\rho''(z_o) \neq 0$.[24] Including also the variation of $\mathcal{F}_4[\rho]$, we learn from eq. (22) that also $p'(\rho_g)$ and thus $\rho''(z_o)$ must be zero. The boundary conditions (27) for the function $p(\rho)$ remain thus the same. The interface profile $\rho(z)$ must, however, be cut at $z=z_o$. This procedure may look somewhat strange, but it is the prize we have to pay for treating a metastable system by a static variational procedure.

The solutions found in this way for ρ_o, ρ_g at various temperatures are shown in figs. 1,2. In fig. 1, the saturation densities ρ_o are given by the crosses along the axis $P = 0$. There is a maximum temperature $T_m = 11.6$ MeV for which the curve $P(\rho)$ touches the abscissa at a finite value of ρ. In the corresponding phase diagram for a finite system, this is the limiting temperature at which the system can exist at zero external pressure in a metastable state. (For experimental values of T_m and the corresponding discussion for classical superheated liquid drops, see Temperley.[18]) In fig. 2, the densities ρ_o and ρ_g obtained

for the metastable case ($P_o = 0$) are shown versus T by the dashed-dotted curves. The density ρ_m at the limiting temperature is seen to be very close to $\frac{1}{2}\rho_\infty$.

In passing we mention that the qualitative features of the curves in figs. 1 and 2 can be obtained by the simplified equation of state

$$P(\rho) = T\rho - a\rho^2 + b\rho^3 \tag{34}$$

with constant parameters a,b. For the critical point at phase equilibrium one finds

$$\rho_{crit} = \frac{a}{3b}\,, \quad T_{crit} = \frac{a^2}{3b}\,, \quad P_{crit} = \frac{a^3}{27b^2}\,. \tag{35}$$

With the saturation density at T = 0 given by $\rho_\infty = a/b$, we find $\rho_{crit} = \rho_\infty/3$ which is closely fulfilled for the SkM* force. For the limiting values of the metastable situation we find

$$\rho_m = \frac{a}{2b} = \frac{1}{2}\rho_\infty\,, \tag{36}$$

which again is very closely fulfilled for the SkM* force, and

$$T_m = \frac{a^2}{4b} = \frac{3}{4}T_{crit}\,; \tag{37}$$

this ratio is not far from $T_m/T_{crit} = 0.79$ found with the SkM* force. The equation of state (34) may thus be used for schematic discussions. We have, however, not used it since it is simple enough to calculate $P(\rho)$ for a Skyrme force exactly.

We have again solved the Euler equation numerically[22] with the boundary conditions (30) - (33). The liquid-drop parameters a_s and a_c corresponding to this metastable situation are shown as functions of the temperature in fig. 4 by the dashed lines. They obviously vanish at the limiting temperature T_m. In an attempt to parametrize the resulting variational density profiles $\rho(z)$, we used the ansatz

$$\rho(z) = \rho_0 \left[e^{z/\alpha - \beta} + \frac{1}{(1+e^{z/\alpha})^{\gamma}} \right]; \quad (z \leq z_c) \qquad (38)$$

the parameter ß was chosen to fulfil eqs. (31) and (32). The parameters α and γ were again determined by minimizing σ eq. (20) with $P_o = 0$. As in the equilibrium case, the values of σ found in this restricted variational calculation were in excellent agreement with those obtained from the exact numerical solutions of $\rho(z)$: the error was less than 1 % for $0 \leq T \lesssim 4$ MeV and less than 0.1 % for $T \gtrsim 5$ MeV.

The fact that the two pairs of curves in fig. 4 ($P_o \neq 0$ and $P_o = 0$, resp.) agree rather accurately for $0 \leq T \lesssim 4$ MeV suggests that the treatment of the gas component for $z > 0$ has little effect on the results at lower temperatures; this is understood by the exponentially small numerical values of either of the ρ_g values up to $T \simeq 4$ MeV (see fig. 2). In fact, even if ρ_g is put artificially equal to zero, one obtains values of a_s and a_c which agree within less than 1 % with those shown in fig. 4 up to $T \simeq 4$ MeV. This shows that up to this temperature the instability of the heated nucleus can be numerically neglected, as it was done in earlier density variational calculations[1]. Similar conclusions were drawn also from HF calculations at T>0[14,15,25].

4. FINITE NUCLEI

Encouraged by the results with the trial density eq. (38) in the semi-infinite case, we are in the process of adapting these variational calculations to finite, isolated nuclei at higher temperatures.[22] The spherical densities are chosen in the form (q = n or p for neutrons or protons)

$$\rho_q(r) = \rho_{oq} \left[e^{\frac{r-R_q}{\alpha_q} - \beta_q} + \frac{1}{\left(1+e^{\frac{r-R_q}{\alpha_q}}\right)^{\gamma_q}} \right] \quad (r \leq R_{cut}) \qquad (39)$$

with, in principle, different values of the parameters α_q, β_q, γ_q, R_q and ρ_{oq} for protons and neutrons. The values of β_q are again determined by requiring

$$\rho_q'(R_{cut}) = 0. \tag{40}$$

Of course, the correct nucleon numbers N and Z are imposed which allows to eliminate e.g. the parameters R_q. The densities are cut at $r = R_{cut}$ which means that the nucleus is put into a spherical box with radius R_{cut}. The free energy

$$F = \int d^3r \, \mathcal{F}[\rho_n(r), \rho_p(r)] \tag{41}$$

is then minimized, subject to the boundary condition (40), with respect to ρ_{oq}, α_q and γ_q for each given R_{cut}. The cut-off radius R_{cut} itself is also determined variationally; it turns out that the free energy F has a maximum at a finite value of R_{cut} for $0 < T \leq T_m^*$ (see sect. 4.1 for the limiting temperature T_m^*). For $T = 0$, $R_{cut} = \infty$ and the densities (39) reduce to generalized Fermi functions used in earlier ETF calculations.[1)] Such simple profiles can, in fact, be used also at moderate temperatures ($T \lesssim 3$ MeV) - thus neglecting the nucleon evaporation - and yield results in excellent agreement[1,3)] with the corresponding earlier HF results.[14)]

4.1 Limiting Temperature Of An Isolated Nucleus

In the context with heavy-ion collisions, there has been some speculation about the maximum amount of excitation energy (or heat) which can be stored in an excited compound nucleus.[26)] The corresponding limiting temperature is expected to be different from T_m obtained in the infinite case (see sect. 3.2) for three reasons:

1) The finiteness of the system. It should not change T_m much for medium or heavy systems.

2) The asymmetry $\rho_n \neq \rho_p$. It is known to lower the critical temperature T_{crit} in the phase equilibrium[27)] and thus presumably also T_m.

3) The Coulomb repulsion. It has the most dramatic effect. In recent HF calculations[25] it was shown to reduce the limiting temperature from $T_m \simeq 12.5$ MeV (for the uncharged nucleus ^{208}Pb) to $T_m \simeq 8$ MeV (for the real ^{208}Pb nucleus).

In Fig. 5 we present results of our calculations for a system with N = Z = 100, omitting the Coulomb interaction. The limiting temperature is found to be close to $T_m = 11.6$ MeV. The densities ρ_g at the cut-off radius are also close to the ones found in the semi-infinite case (see Fig. 2).

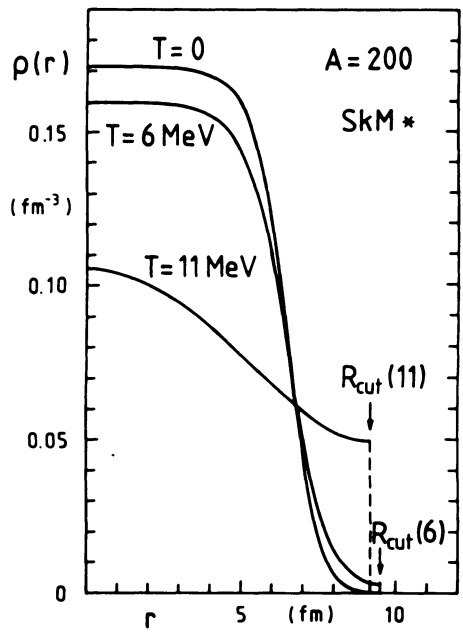

Figure 5:
Variational density profiles eq. (39) for a nucleus with N = Z = 100 (no Coulomb interaction) obtained with the SkM* force. From ref.[22].

Calculations with asymmetric nuclei including the Coulomb force are in progress.[22] As a preliminary result, we find for ^{208}Pb a limiting temperature

$$8 \text{ MeV} \lesssim T_m^* \lesssim 8.5 \text{ MeV} \quad (^{208}\text{Pb}) \tag{42}$$

with the SkM* force. Beyond this temperature, no minimum could be found for the free energy F eq. (41) for any stationary value of R_{cut}: the

system ceases to be bound. The reason for this instability is clearly the Coulomb repulsion (see also refs.[25,28]). Real nuclei will therefore not reach any liquid-to-gas phase transition point.[26]

The result eq. (42) is in close agreement with that found by Bonche et al.[25] in their HF calculations, although they used a Skyrme force (SkM) with a lower surface tension[1,20] which thus should lead to lower limiting temperatures. A higher value of T_m^* would be explained by the different boundary conditions used in ref.[25] which, in fact, seem to be closer to those of a phase-equilibrium situation.

Our results allow a simple estimation of the evaporation time of the metastable nucleus. The finite gas density $\rho_g = \rho(R_{cut})$ at the confining wall corresponds to a gas pressure P_g which, for the small values of ρ_g found for $T \lesssim 6$ MeV, is that of an ideal gas:

$$P_g \simeq T\rho_g . \tag{43}$$

Using the equipartition law, this corresponds to an average radial velocity

$$\bar{v}_r = \sqrt{P_g/m\rho_g} \simeq \sqrt{T/m} \tag{44}$$

with which the nucleons knock at the wall at R_{cut}. If the wall were released, they would escape with a flux $j_r = \rho_g \bar{v}_r$ through the surface $4\pi R_{cut}^2$, giving an evaporation rate

$$\frac{dN}{dt} \approx 4\pi R_{cut}^2 \rho_g \sqrt{T/m} . \tag{45}$$

From our preliminary results for ^{208}Pb at T = 8 MeV, we obtain in this way an evaporation time of $\tau_{evap.} \simeq 1.5 \times 10^{-24}$ sec which is clearly unphysical. This means that the mean-field approach is no longer consistent at such temperatures. In order to have $\tau_{evap.} \gtrsim 10^{-22}$ sec, T should stay below $\sim$ 5 MeV. We thus draw the preliminary conclusion that real nuclei will hardly exist beyond T $\simeq$ 5 MeV since then the mean field no longer exists. To be more cautious: In a static meanfield approach, we cannot predict the existence of finite, metastable nuclei with temperatures higher than T $\approx$ 5 MeV.

4.2 Other Applications

We finally mention very briefly two applications of the finite temperature ETF theory to finite nuclei at temperatures $T \lesssim 4$ MeV where the gas component was neglected ($\rho_g = 0$). Static deformation energies were calculated and temperature-dependent fission barriers were obtained in refs.[1,3] As a first step towards nuclear dynamics, sum rules and energies of giant monopole and dipole resonances were calculated as functions of the temperature[29]. The newest results of both kinds of calculations will be presented at the conference.

REFERENCES

1) Brack, M., Guet, C. and Håkansson, H.-B., Physics Reports 123(5), 275(1985).

2) Guet, C., Håkansson, H.-B. and Brack, M., Phys. Lett. 97B,7(1980).

3) Brack, M., J. Phys. (Paris) Colloques C6-15(1984); Phys. Rev. Lett. 53,119(1984) and 54,851(1985).

4) Bartel, J., Brack, M. and Durand, M., Nucl. Phys. A445,263(1985).

5) Wigner, E.P., Phys. Rev. 40,749(1932); Kirkwood, J.G., Phys. Rev. 44,31(1933).

6) Kirzhnits, D.A., "Field Theoretical Methods in Many Body Systems" (Pergamon, Oxford, 1967).

7) Grammaticos, B. and Voros, A., Ann. of Phys. 123,359(1979) and 129,153(1980).

8) Hodges, C.H., Can. J. Phys. 51,1428(1973).

9) Hohenberg, P. and Kohn, W., Phys. Rev. 136,B864(1964).

10) Mermin, N.D., Phys. Rev. 137,A1441(1965).

11) Brack, M., Jennings, B.K. and Chu, Y.H., Phys. Lett. 65B,1(1976).

12) Guet, C. and Brack, M., Z. Phys. A 297,247(1980).

13) Brack, M. and Bartel, J., Proc. of 4th Int. Conf. on Recent Progress in Many Body Theories, San Francisco 1985 (Eds. P. Siemens and R. Smith).

14) Brack, M. and Quentin, P., Phys. Lett. 52B,159(1974); Physica Scripta A10,163(1974).

15) Mosel, U., Zint, P. and Passler, K.H., Nucl. Phys. A236,252(1974).

16) Skyrme, T.R., Phil.Mag. 1,1043(1956); Nucl. Phys. 9,615(1959); Vautherin, D. and Brink, D.M., Phys. Rev. C5,626(1972).

17) Negele, J.W. and Vautherin, D., Phys. Rev. C5,1472(1972); Campi, X. and Bouyssy, A., Phys. Lett. 73B,263(1978).

18) Temperley, H.N.V., Proc. Phys. Soc. 59,199(1947).

19) Ravenhall, D.G. et al., Nucl. Phys. A 405,571(1983).

20) Bartel, J. et al., Nucl. Phys. A 386,79(1982).

21) Myers, W.D., and Swiateck, W.J., Ann. of Phys. 55,395(1969).

22) Strumberger, E. and Brack, M., to be published.

23) Stocker, W. and Burzlaff, J., Nucl. Phys. A 202,265(1973).

24) Barranco, M. and Treiner, J., Nucl. Phys. A 351,269(1981).

25) Bonche, P., Levit, S. and Vautherin, D., Nucl. Phys. A427,278(1984); A 436,265(1985).

26) Panagiotou, A.D. et al., Phys. Rev. Lett. 52,496(1984); Siemens, P., Nature 305,410(1983); Nucl. Phys. A 428,197c(1984).

27) Lamb, D.Q. et al., Nucl. Phys. A 360, 459 (1981).

28) Levit, S. and Bonche, P., Nucl. Phys. A 437,426(1985).

29) Meyer, J., Quentin, P. and Brack, M., Phys. Lett. 133B,279(1983).